Cellular and Molecular Bioengineering, Vol. 2, No. 3, September 2009 *(© 2009)* pp. 375–385
DOI: 10.1007/s12195-009-0067-5

Systemic Analysis of Tumor Cell-Induced Endothelial Calcium Signaling and Junction Disassembly

HSIN-HSIN PENG and CHENG DONG

Department of Bioengineering, Pennsylvania State University, 233 Hallowell Bldg., University Park, PA 16802, USA

(Received 11 May 2009; accepted 3 July 2009; published online 16 July 2009)

Abstract—It has been shown in our previous study that melanoma cells induce junction disassembly in the manner related to phospholipase C-calcium activation. In light of this observation, we have developed a mathematical model of the signaling pathway and adapted multi-parametric sensitivity analysis (MPSA) to identify important parameters in the model, which examines tumor cell-induced calcium mobilization in endothelial cells. The objective functions, with respect to individual parameters, were generated for the calcium mobilization model and MPSA was performed according to the function. The results showed that sarco/endoplasmic reticulum calcium ATPase was one of the putative key factors in regulating calcium mobilization. The model is a proof of concept of systemic analysis of a signaling network, and the results may have practical applications in describing how endothelial cells respond to tumor cells. Taken together, we have devised numerical means to macroscopically study roles of calcium signaling in endothelial cells in contact with metastatic tumor cells.

Keywords—Multi-parametric sensitivity analysis, Melanoma, VE-cadherin.

INTRODUCTION

Metastatic tumor cell-associated signaling events have not been extensively studied. Such events as endothelial junction regulation, for example, may result in changes in the microenvironment favoring migrating tumor cells. Transmigration of tumor cells through endothelial cells (ECs) requires a loss of endothelial junction integrity. It is therefore imperative that we understand the signaling pathways leading to the redistribution of endothelial junctions and subsequent tumor transmigration. In this study, we characterized signals initiated by melanoma cells consequential for regulation of interendothelial adherens junctions and transvascular migration of tumor cells.

Address correspondence to Cheng Dong, Department of Bioengineering, Pennsylvania State University, 233 Hallowell Bldg., University Park, PA 16802, USA. Electronic mail: cxd23@psu.edu

One signaling pathway of interest is the group of calcium-dependent signaling cascades, a diverse series of signaling events that center on induction or regulation of intracellular calcium ($[Ca^{2+}]_i$) for propagation of signaling cascades and alternation of biological functions. It is reported that the regulation of endothelial integrity is mediated through a $[Ca^{2+}]_i$-dependent mechanism upon endothelial cell exposure to hydrogen peroxide.[14] The rise in $[Ca^{2+}]_i$ level is transient and upstream of the signaling pathway compromising endothelial integrity. In addition, thrombin binds to its receptor inducing calcium influx to cause cytoskeletal rearrangement.[13] Endothelial $[Ca^{2+}]_i$-dependent signaling pathways can also be elicited by leukocytes undergoing transendothelial migration.[7] Furthermore, we have previously shown that malignant tumor cells can regulate endothelial junction integrity by recruiting classical calcium release in endothelium.[12] Therefore, development of a calcium signaling model would be beneficial for understanding the mechanisms of endothelial junction modulation.

Cellular processes are modulated through complex interactions involving a large number of proteins and transcription factors; therefore, computational approaches such as differential equation modeling and enzyme kinetic modeling, in addition to biological investigations, are complementary for studying intracellular dynamics.[2–4] Schemes of the enzymatic reaction can be used to represent protein–protein interactions and protein degradation for developing models of the signaling pathway.[2] The standard Michaelis–Menten equation: $E + S \leftrightarrow ES \rightarrow E + P$, derived from the general enzymatic reaction, can be considered as two sequential reactions in the signaling transduction cascades. E denotes the concentration of an enzyme that binds a substrate (S) to form an enzyme–substrate complex (ES) with rate coefficient k_1. The reversible intermediate state ES can then either dissociate to E and S with rate coefficient k_2, or carry the reaction to completion with reaction product, P, and regenerated enzyme, E, with rate coefficient k_3. The theoretical

model of a signaling transduction network can be constructed mathematically from existing data as analogs of enzymatic reactions. The corresponding ordinary differential equations (ODEs) of reaction rates for each component in the cascade can then be generated.[2]

In this study, we established a mathematical model to describe intracellular calcium mobilization in the context of tumor metastasis. To take into account dynamic changes of the biological system as system parameters vary, we employed a multi-parametric sensitivity analysis (MPSA), previously presented by Cho *et al.* for identifying key parameters in a signaling pathway model.[4] Briefly, an objective function, defined as a sum of square errors between observed and perturbed values, could describe how much the model output changes from an observed data in relation to the perturbation of parameters. An objective function smaller than the average of the objective function, was classified as acceptable; otherwise it was classified as being in an unacceptable range. By correlating the distribution of the parameter values to acceptable and unacceptable results, the parametric sensitivity could be then evaluated.[4] The MPSA approach could be adapted to analyze signaling processes and identify key parameters in the process. The capability of this network modeling enables quantitative analysis of cellular interactions and exploration of molecular targets for follow-up studies.

MATERIALS AND METHODS

Cell Culture and $[Ca^{2+}]_i$ Ratiometric Measurement

Human umbilical vein endothelial cells (HUVECs; American Type Culture Collection, Manassas, VA) were cultured in Ham's F12-K media (Biofluids Inc., Gaithersberg, MD) supplemented with 10% FBS (Biofluids Inc.), 10 μg/mL endothelial cell growth supplement (Sigma Chemical Co., St. Louis, MO), 100 μg/mL heparin (Sigma Chemical Co.), 100 units/mL penicillin–streptomycin (Biofluids Inc.) at 37 °C under 5% CO_2. Melanoma cell line A2058 were obtained from NCI (NIH, Bethesda, MD) and maintained in DMEM (Biofluids Inc.) supplemented with 10% FBS.

For $[Ca^{2+}]_i$ assays, HUVECs were incubated with 10 μM Fura-2-AM (Invitrogen Molecular Probes, Inc., Eugene, OR) for 30 min. The detailed procedure for a $[Ca^{2+}]_i$ ratiometric assay is described elsewhere.[6,12] In brief, a computer software package was used to control the excitation light (340 and 380 nm band pass filters), sample and record the emitted fluorescence (510 nm) images from the Fura-2-AM loaded cells once every 6 s. Ratio images of the cells at rest were recorded for the first 100 s to establish a $[Ca^{2+}]_i$ baseline. Melanoma cell suspension was perfused into the chamber with a syringe connected to a tubing and raw images were collected for four additional minutes. As a negative control, polystyrene microspheres (Polyscience, Inc., Warrington, PA) were used to simulate cellular volumes in suspension. For treatment of phospholipase C (PLC) inhibitor, endothelial cells were exposed to 10 μM U73122 (Sigma Chemical Co.) for 5 min prior to the addition of melanoma cells to endothelial cells.

Immunofluorescence Staining

Cells were fixed using 5% formaldehyde in PBS for 15 min at room temperature and washed three times in PBS. Fixed cells were treated for 20 min with 0.3% Triton X-100, 5% calf serum (CS), and 2.5% goat serum (GS) in PBS and exposed to 1 μg of primary antibody (anti-vascular endothelial (VE)-cadherin; mouse monoclonal IgG1; Santa Cruz Biotechnology, Santa Cruz, CA) in PBS with 0.3% Triton X-100/5% CS/2.5% GS overnight at 4 °C. Secondary antibody (AlexaFluor-488 conjugated goat anti-mouse IgG; Invitrogen Molecular Probes, Inc.) was applied at concentration of 1 μg/mL in PBS with 5% CS/2.5% GS, and incubated at 4 °C for 1 h. The immunofluorescence stained plates were observed using an Olympus IX51 fluorescence microscope (Olympus Inc., Tokyo, Japan) at excitation/emission wavelengths of 488 nm/520 nm, respectively. Digital images were taken and Image J 1.37v (NIH, Bethesda, MD) was used to quantify junction disassembly. Area of disassembly was defined as area of open space between adjacent cells. It was visualized as patches of distinctively darker area in contrast to the fluorescence-labeled adherent cells in the image. For quantification, the area of disassembly was identified manually and the pixels within the identified area were tallied. The ratio of area of disassembly over total area of the image was thus defined as the ratio of total number of pixels within the identified area of disassembly vs. total number of pixels of the entire image. For treatment of PLC inhibitor, endothelial cells were treated with 10 μM U73122 for 5 min prior to melanoma addition.

Transendothelial Migration

The transendothelial migration assay was performed as previously described.[12] For some experiments, monolayers were pretreated with 10 μM U73122 for 5 min or 2.6 μM Gö6976, a protein kinase C (PKC) inhibitor, for 30 min. Next, the drug-containing medium was replaced and the filter was washed with fresh assay medium three times prior to

melanoma cell addition. Melanoma cell transendothelial migration was evaluated by tallying the number of cells migrated to the lower side of the membrane as viewed under 10× magnification. Seven fields of a filter were quantified and averaged. At least three filters were independently analyzed.

Establishment of Calcium Signaling Model

A graphical template of the classical calcium signaling pathway including concentration variables, such as PLC, phosphatidylinositol bisphosphate (PIP_2), diacylglycerol (DAG), PKC, inositol-1, 4, 5-triphosphate (IP_3), IP_3 receptor (IP_3R), calcium and calmodulin (CaM) coupling and sarco/endoplasmic reticulum calcium-ATPase (SERCA), etc. and kinetic parameters, was established. A central process of the signaling cascade was the release of calcium from endoplasmic reticulum (ER) via IP_3. IP_3 and DAG were produced from PIP_2 cleavage via G protein-coupled receptor (GPCR)-linked PLC activation. For the purpose of the model, they were represented by the following equations:

$$\begin{aligned}
&G + PLC \overset{k_1,k_2}{\longleftrightarrow} PLC_G\\
&PLC_G + PIP_2 \overset{k_3,k_4}{\longleftrightarrow} PIP_2_PLC_G\\
&PIP_2_PLC_G \overset{k_5}{\rightarrow} PLC_G + DAG + IP_3\\
&3IP_3 + IP_3R \overset{k_{10},k_{11}}{\longleftrightarrow} IP_3R^*\\
&IP_3R^* \overset{k_{12}}{\rightarrow} Ca^{2+}
\end{aligned}$$

The G protein that interacted with PLC leading to the production of G protein and PLC complex was expressed as G + PLC ↔ PLC_G. In addition, the stable open conformation of the receptor required activation by at least three IP_3 molecules,[10] so this process was formulated as $3IP_3 + IP_3R \leftrightarrow IP_3R^*$ (* denotes an active form).

The model described above was next linked to a prototypical process downstream of calcium-flux signals, involving complexes of Ca^{2+}–CaM binding to myosin light chain kinase (MLCK), as shown in the following equations:

$$\begin{aligned}
&CaM + 4Ca^{2+} \overset{k_{13},k_{14}}{\longleftrightarrow} Ca^{2+}_CaM\\
&Ca^{2+}_CaM + MLCK \overset{k_{15},k_{16}}{\longleftrightarrow} MLCK_Ca_CaM\\
&Ca^{2+} + SERCA \overset{k_{17},k_{18}}{\longleftrightarrow} Ca^{2+}_SERCA\\
&Ca^{2+}_SERCA \overset{k_{19}}{\rightarrow} Ca^{2+}\ store\\
&Ca^{2+}_ext \overset{k_{20}}{\rightarrow} Ca^{2+}
\end{aligned}$$

CaM is an important target of Ca^{2+}-mediated signaling. Up to four calcium ions can bind to CaM in a Ca^{2+}–CaM complex; the reaction was therefore expressed as $CaM + 4Ca^{2+} \leftrightarrow Ca^{2+}\_CaM$. In addition, a calcium gradient across the ER membrane was maintained by active pumping through SERCA. The process can then be formulated as $Ca^{2+} + SERCA \leftrightarrow Ca^{2+}\_SERCA \rightarrow Ca^{2+}$ store. Moreover, extracellular Ca^{2+} influx was incorporated into the simulation by adding Ca^{2+}_ext into the model.

ODEs Formulation and Sensitive Analysis

The rate of concentration changes was expressed as a time derivative (dc/dt; c denotes concentration of the variable). A range of initial concentrations for some of the variables was also tested. All numerical simulations of biological reaction and ODEs were processed in MATLAB 7.1 (MathWorks, Natick, MA).

$[Ca^{2+}]_i$ simulations with variations in single parameters were performed for local sensitivity analysis. For MPSA, paired parameters k_i were chosen and objective function of $[Ca^{2+}]_i$ was calculated with respect to the parameters. When the objective function values are larger than the overall average, they indicate greater-than-acceptable differences from the actual values. The corresponding correlation coefficient of cumulative acceptable or unacceptable frequency was calculated and compared as described by Cho *et al.*[4] A smaller correlation coefficient indicates greater sensitivity of the parameter to perturbations of the system.

RESULTS

Endothelial Responses upon Melanoma Cell Contact

We have previously demonstrated a transient rise in endothelial $[Ca^{2+}]_i$ elicited by melanoma cell interaction with the epithelium. The rise of calcium flux consisted of a single peak that gradually fell back to baseline with progression of time.[12] This single-peak profile was characteristic of the calcium influx observed, as was confirmed by tests determining whether oscillation occurred at all (Fig. 1a). Perfusion of polystyrene microspheres did not induce $[Ca^{2+}]_i$ response (data not shown), indicating that physical agitation caused by addition of microspherical suspension is not sufficient for triggering responses. To assess the role of PLC, HUVECs were pretreated with PLC inhibitor U73122 at 10 μM that resulted in complete attenuation of the cell responding, as well as depressed magnitude of peak $[Ca^{2+}]_i$ (Fig. 1b).

In addition, the melanoma-mediated induction of the classical Ca^{2+} release led to redistribution of endothelial junction. As shown in Fig. 2a, a continuous pattern of VE-cadherin staining was detected in the periphery of endothelial cells in the absence of melanoma cells. Addition of melanoma cells resulted in a diffuse VE-cadherin staining at the site of melanoma

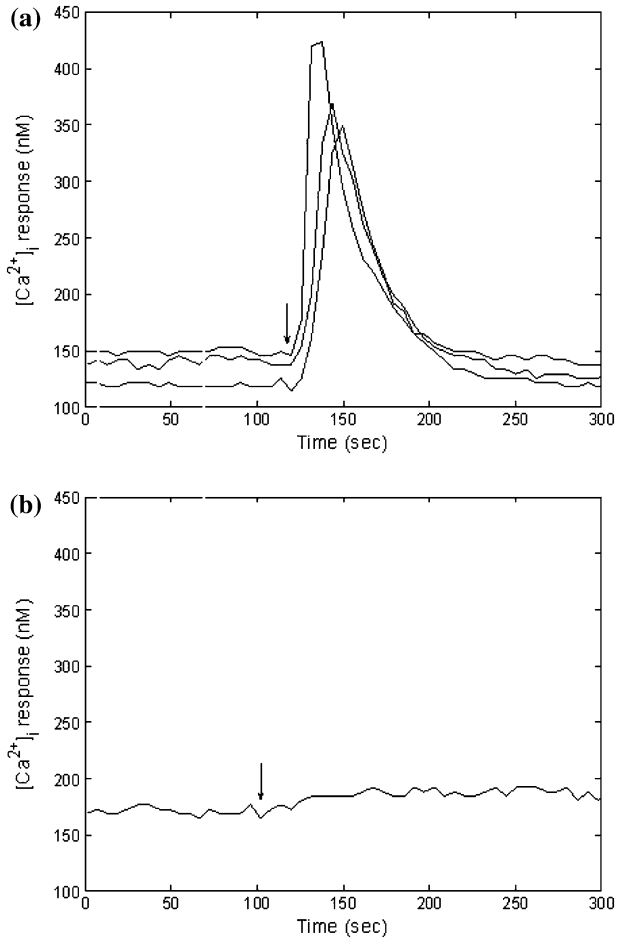

FIGURE 1. (a) Melanoma-induced transient calcium response in endothelial cells. Calcium responses of three cells were measured. The result was representative of 11 independent experiments. (b) Endothelial cells treated with U73122, completely attenuated calcium response. Arrow indicates the time at which melanoma cells were added. The result was representative of 3 independent experiments.

cell contact after 45 min of co-culture (Fig. 2b) and the diffuse staining patterns were rescued by PLC inhibitor (Fig. 2c). For quantitative analysis, percentage of VE-cadherin disassembly within an image was calculated. A2058 melanoma cells induced 17 ± 2% of VE-cadherin dissociation as measured in the image (A2058 + EC), while the image of the negative control, EC monolayer, showed intact VE-cadherin (0.02% disassembly) (Fig. 2d). Pretreatment of U73122 reduced melanoma cell-associated gap formation to 3 ± 1% on EC (A2058 + U73122-treated EC; $p < 0.01$). Therefore, melanoma cells induce reorganization of VE-cadherin through PLC-dependent mechanism. The quantitative measurement further provides the means for quantitative comparison besides qualitative observation via experimentation.

We were also interested in determining the functional significance of PLC, Ca^{2+} induction, and PKC in altering melanoma transendothelial migration. We previously utilized the Boyden migration assay system in which a confluent monolayer of HUVEC was seeded on the upper surface of the fibronectin-coated filter and melanoma chemotaxis through the monolayer toward type IV collagen in the bottom wells was examined.[11] Melanoma cells transmigrated through untreated or treated endothelial cells with 10 μM U73122 or 2.6 μM Gö6976 as shown in Fig. 3. Values were calculated as percentages (of the control case) in which melanoma migrated through untreated endothelium (A2058 + untreated EC). Pretreatment with U73122 or Gö6976 inhibited transmigration by 37 ± 3% (A2058 + U73122-treated EC; $p < 0.001$) or 39 ± 6% (A2058 + Gö6976-treated EC; $p < 0.001$), respectively.

Simulation of the Calcium Signaling Processes

Figure 4 illustrates the melanoma-induced $[Ca^{2+}]_i$ signaling cascades in endothelial cells responsible for initiating junction disassembly and melanoma migration in the manner related to PLC/IP_3 activations and release of calcium from its intracellular stores in the ER. In addition, PKC and MLCK were suggested to be a downstream targets of the pathway linked to the Ca^{2+}–CaM-dependent mechanism. Based on the experimental finding, a graphical template of the calcium pathway was established as shown in Appendix A. Circles represent concentration variables, and k_i (i = 1–20) are the kinetic parameters. Solid arrows indicate the forward reactions and dashed arrows indicate the reverse reactions. The rates of concentration changes were formulated in Appendix B. The parameter values used to solve the ODEs were obtained from the literature[1,9] and Database of Quantitative Cellular Signaling[15] as summarized in Appendix C. The assigned initial concentrations are listed in Appendix D. In the simulation, binding of ligand to GPCR increased the levels of IP_3 and $[Ca^{2+}]_i$. As shown in Fig. 5, at an assigned initial concentration of 18 μM for this simulation, PLC induced a Ca^{2+} influx that peaked at 430 nM. The $[Ca^{2+}]_i$ output was limited by the IP_3 production that maxmized at 2.3 μM in this scenario. In order to further address the role of PLC in $[Ca^{2+}]_i$ response, a range of additional initial concentrations of PLC was assigned in $[Ca^{2+}]_i$ simulation. The Ca^{2+} was relatively insensitive to PLC at an initial concentration greater than 15 μM with a fixed G protein concentration (Fig. 6a). Figure 6b shows the change of peak $[Ca^{2+}]_i$ in a [PLC]-dependent manner. Peak $[Ca^{2+}]_i$ was nonlinearly proportional to smaller [PLC] and saturated at higher [PLC]. Reducing the PLC below 2 μM resulted in no rise in $[Ca^{2+}]_i$.

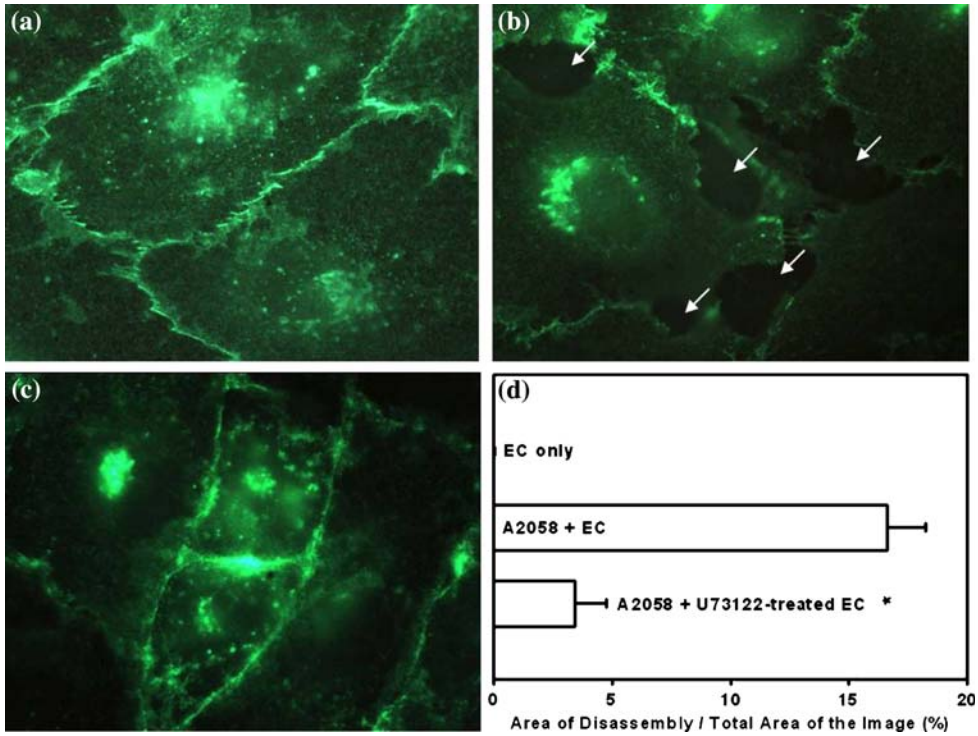

FIGURE 2. (a) A continuous VE-cadherin staining pattern in endothelial cells. VE-cadherin was also detected along perinuclear organelles intracellularly. (b) Loss of VE-cadherin expression was caused by melanoma cell contact after 45 min. Arrows indicate the sites where gaps formed. (c) A majority of VE-cadherin remained continuous after 45 min when pretreated with PLC inhibitor. (d) Quantification of endothelial junction disassembly. Pixels within the area of disassembly were quantified as a percentage of the total image area, defined as pixels within area of disassembly/total pixels of the image. Results are presented with mean ± SEM; *n* = 6–19.

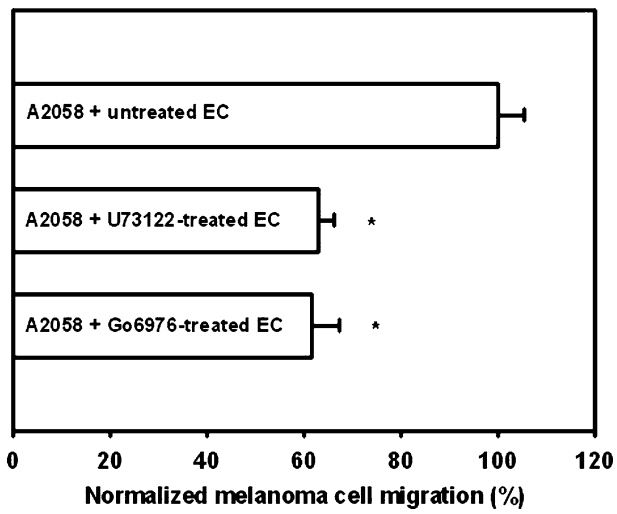

FIGURE 3. PLC and PKC signals were required for melanoma cell transendothelial migration. Results are presented with mean ± SEM; *n* = 3–5.

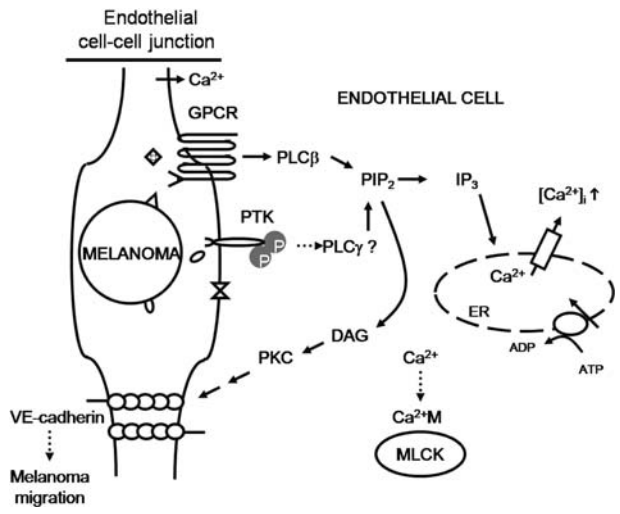

FIGURE 4. Schematic diagram of calcium signaling pathway initiated by melanoma contact to endothelium. Arrows indicate the direct signals and dashed arrows indicate tentative signals.

Local Sensitivity Analysis for $[Ca^{2+}]_i$ Response

The $[Ca^{2+}]_i$ response with respect to each single parameter change was evaluated and compared by local sensitivity analysis. For instance, perturbation of G protein/PLC association rate coefficient k_1 and Ca^{2+} uptake rate constant k_{19} showed distinct effects

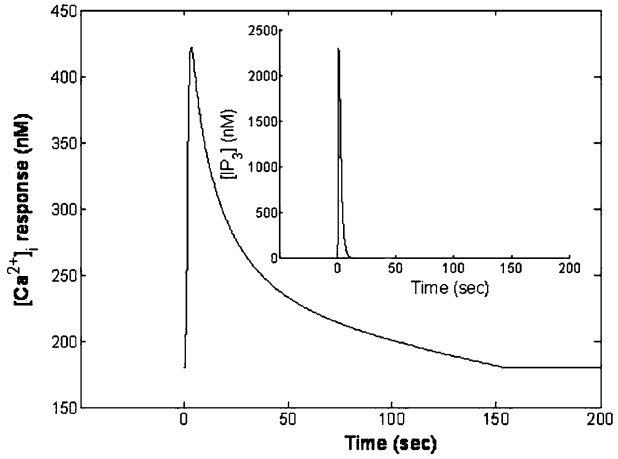

FIGURE 5. Simulation result of $[Ca^{2+}]_i$ response. Inserted plot is the $[IP_3]$ response over time.

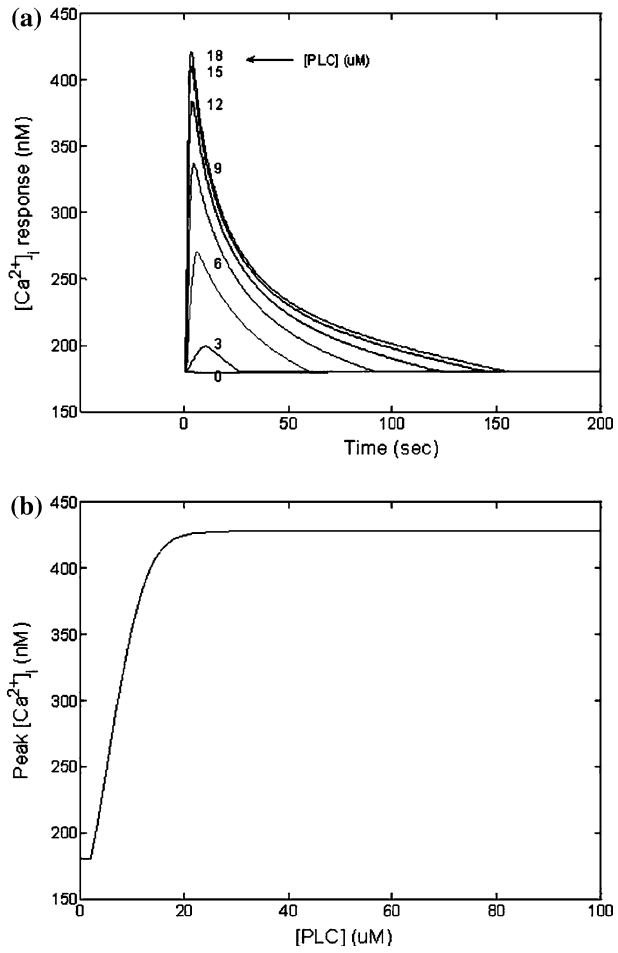

FIGURE 6. Effect of different initial concentrations of PLC on $[Ca^{2+}]_i$ response. (a) Changes in $[Ca^{2+}]_i$ in response to [PLC] with a range between 0 and 18 μM. (b) PLC produced a concentration dependent-peak $[Ca^{2+}]_i$ response.

on $[Ca^{2+}]_i$ output (Fig. 7). Whereas $[Ca^{2+}]_i$ was relatively insensitive to variations of k_1, it responded more on perturbation of k_{19}. The Ca^{2+} influx decreased as

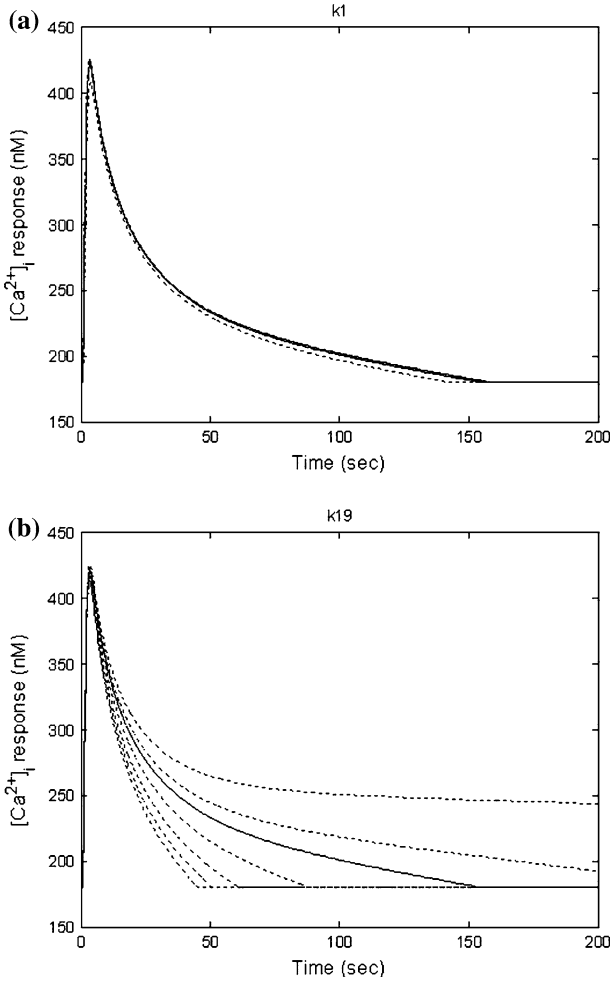

FIGURE 7. The time course of $[Ca^{2+}]_i$ response with respect to the variation of (a) k_1 and (b) k_{19}. The solid line represents a simulated $[Ca^{2+}]_i$ response using the reference parameter value and the dashed line represents $[Ca^{2+}]_i$ responses for various parameter values from one-fifth to five times reference value. The Ca^{2+} influx decreased as k_{19} increased.

k_{19} increased. The data suggest that rate of Ca^{2+} uptake via SERCA greatly affects the robustness of cellular machinery of calcium signaling.

Objective Function of $[Ca^{2+}]_i$ and Key Parameters in the Calcium Signaling Pathway

In order to determine the importance of simultaneous variations for multiple parameters in a signaling transduction pathway, a MPSA was performed to select the most sensitive parameters by calculating $[Ca^{2+}]_i$ objective function with respect to k varying from one-fifth to five times the assigned value. For instance, k_3, the PLC_G/PIP_2 association rate coefficient, and k_5, the rate constant for production of DAG and IP_3 from PIP_2_PLC_G, were selected for

comparison; the ranges of variations were set to be $k_3 \in [0.166, 4.15]$ and $k_5 \in [0.116, 2.9]$ with other parameter values fixed. Figure 8 shows the resulting objective function of $[Ca^{2+}]_i$ with respect to k_3 and k_5. The objective function values smaller than the overall average of the objective function (2.789×10^6 nM^2) were classified as acceptable; values larger than the average were said to be within an unacceptable range.

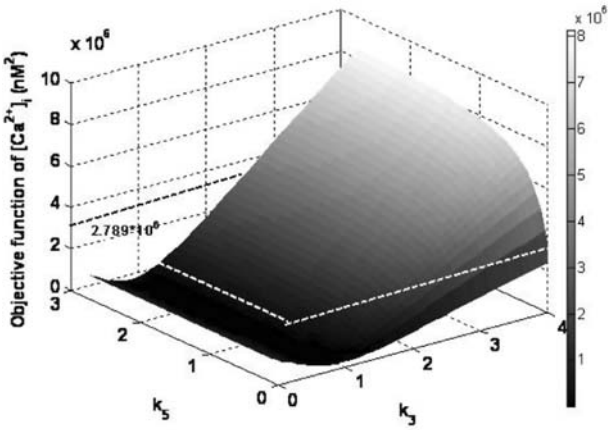

FIGURE 8. Objective function of $[Ca^{2+}]_i$ distribution with respect to k_3 and k_5. The value of the objective function smaller than 2.789×10^6 (represented by dashed line) was considered to be acceptable.

Acceptable and unacceptable frequencies of the parameters were computed and corresponding correlation coefficients of cumulative frequencies were evaluated. Figures 9a and 9b show the distribution of the acceptable and unacceptable frequencies for k_3 and k_5; Figs. 9c and 9d represent the cumulative acceptable and unacceptable frequencies. The corresponding correlation coefficients were computed to be 0.650 for k_3 and 0.999 for k_5. Therefore, the cumulative frequencies of acceptable and unacceptable instances for the parameter k_3 differ more than that for k_5, so k_3 is more sensitive than k_5.

The MPSA was performed for the parameters that have been shown to play a role in the $[Ca^{2+}]_i$ regulation, such as G protein/PLC association rate coefficient k_1, PLC_G/PIP_2 association rate coefficient k_3, DAG and IP_3 formation rate constant k_5, IP_3/IP_3R association rate constant k_{10}, Ca^{2+}/CaM association rate constant k_{13}, and Ca^{2+} uptake rate constant k_{19}. The parameters were paired and calculated based on the statistical difference in terms of correlation coefficient of the acceptable and unacceptable cumulative

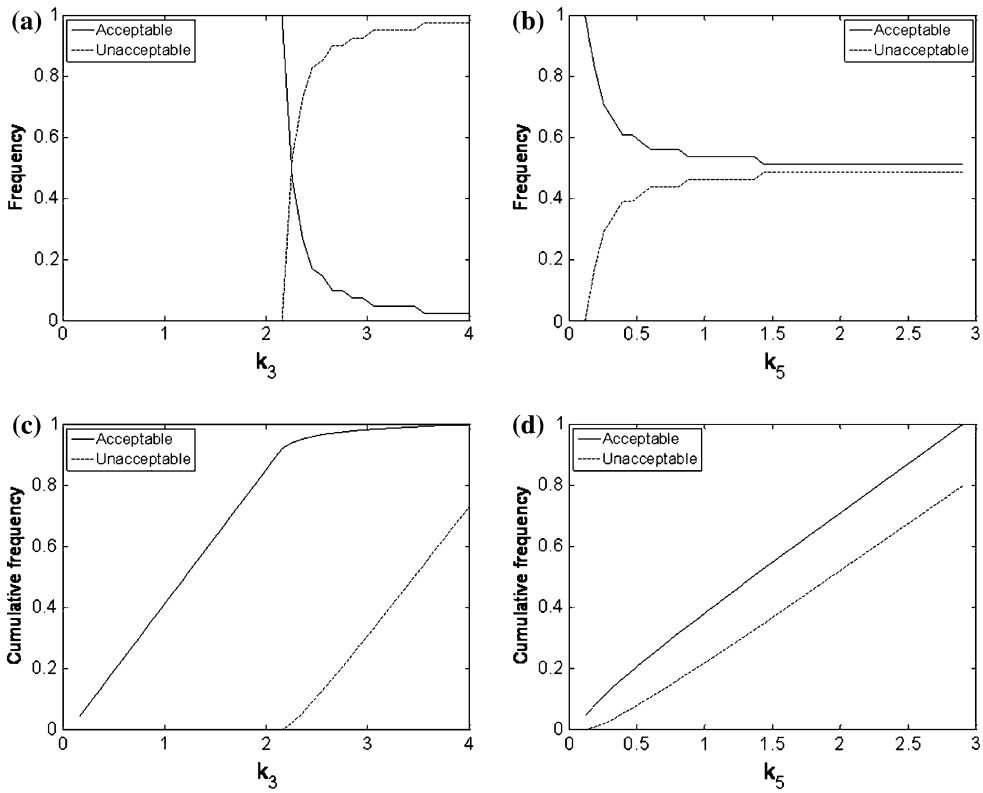

FIGURE 9. Distribution of objective function of acceptable and unacceptable frequencies for (a) k_3 and (b) k_5. Correlation coefficients of cumulative acceptable and unacceptable frequencies for (c) k_3 and (d) k_5 were 0.650 and 0.999, respectively. The solid line denotes the frequencies in the acceptable range and dashed line denotes the frequencies in the unacceptable range.

TABLE 1. Paired k_i (i = 1, 3, 5, 10, 13, and 19) for MPSA and their correlation coefficients of cumulative acceptable and unacceptable frequencies.

	k_1	k_3	k_5	k_{10}	k_{13}	k_{19}
k_1	–	0.000	1.000	1.000	NaN	0.000
k_3	0.494	–	0.999	0.999	0.489	0.598
k_5	0.597	0.650	–	0.832	0.829	0.809
k_{10}	0.597	0.641	0.891	–	0.887	0.874
k_{13}	0.592	0.628	0.864	0.803	–	0.715
k_{19}	0.572	0.713	0.849	0.798	0.945	–

frequencies. As shown in Table 1, the correlation coefficient of the cumulative frequency distributions for k_{19} was smaller than those of k_1, k_3, k_5, and k_{13}; that of k_{13} smaller than those of k_3 and k_5; that of k_{10} smaller than that of k_5; that of k_3 smaller than those of k_1, k_5, and k_{10}; that of k_1 smaller than those of k_5 and k_{10}. The correlation coefficients of the cumulative frequency distributions for k_{19} and k_{10} were comparable, as were those of k_{13} and k_{10}. Therefore, k_{19} were determined to be most sensitive in the model, implicating that the $[Ca^{2+}]_i$ may be most dependent on the rate of Ca^{2+}-uptake via SERCA. In addition, PLC_G/PIP_2 and Ca^{2+}/CaM productions were also shown to be sensitive for $[Ca^{2+}]_i$.

DISCUSSION

Tumor cells induce a series of signals during their interactions with the host environment in order to facilitate their transmigration. The way in which host cells respond to tumor invasion is regulated through signal transduction and the resultant alteration of cellular activities. The signals initiated by melanoma cells regulating endothelial adherens junctions and transmigration have been characterized in this study. We have identified the signaling factors, including PLC, Ca^{2+} influx and PKC that have roles in regulating EC junctions and melanoma transendothelial migration. In addition, we have created a model that employed minimal components to quantitatively describe and simulate Ca^{2+} mobilization on the basis of enzymatic reactions. We were able to assess parameter variations as responses to any perturbations of the initial concentrations or parameters in the GPCR-mediated Ca^{2+} signaling pathway.

Intracellular signaling regulates cell function in response to external stimuli. We have shown that PLC–Ca^{2+} is an important pathway for melanoma-associated VE-cadherin junction disassembly. However, minor gap formations were observed on the interendothelial junction of U73122-pretreated endothelium, indicating that other pathways also play a role in signaling VE-cadherin reorganization. P38 mitogen-activated protein kinase (MAPK) has been suggested as an important upstream component in relation to VE-cadherin regulation.[11] The pathways, such as the Ca^{2+} signaling, MAPK cascades, and transcriptional machinery, may cross talk and form networks.[8,16] Therefore, there is an increasing need to express biological interactions systematically as mathematical models, in order to take advantage of the ability of models to process and analyze simultaneously parameters and variables. Through construction of each signaling component, a signaling pathway can be completely modeled, and the resultant model can be adopted for simulating other similar signaling pathways. Here we modeled a classical Ca^{2+} signaling pathway with the parameter values obtained from literature and online databases.[1,15] This model of Ca^{2+} mobilization in endothelial cells in contact with tumor cells consisted of elementary Ca^{2+}-related components including G protein complex, PLC activation, generation of DAG and IP_3 followed by IP_3-mediated intracellular Ca^{2+} fluxes, and SERCA activity. In addition, cytoplasmic regulatory components, CaM complexes and MLCK, were also included in the model. The results of simulation revealed the single-peak behavior of a transient $[Ca^{2+}]_i$ signaling process that was consistent to that observed for the melanoma-recruited endothelial $[Ca^{2+}]_i$ mobilization.[12] In some of the scenarios of the IP_3-generated Ca^{2+}-mobilization models, $[Ca^{2+}]_i$ were allowed to oscillate, while in other scenarios it was held steady, which reflects the wide diversity of the nature of this phenomenon.[5,9] Furthermore, we have considered the capacitative Ca^{2+} entry by adding Ca^{2+}_ext into the model. In addition to $[Ca^{2+}]_i$ simulation, other second messengers such as IP_3 and DAG, intermediate molecules connected to the Ca^{2+} signal, could also be presented simultaneously.

Network modeling provided a facile tool to describe the Ca^{2+} signaling process in quantitative terms. Any variable and parameter could be manipulated to evaluate how the change of components in the system would affect the endpoints. In most simulations, $[IP_3]$ and $[Ca^{2+}]_i$ were suppressed at the low value of forward rate constants. Initial concentrations of G protein complex, PLC, PIP_2, IP_3R would also influence the downstream outputs (data not shown). Local sensitivity analysis was used to evaluate the signaling pathway model with respect to a one parameter change for identifying key molecules. We showed that calcium uptake rate was crucial to the Ca^{2+} influx process by virtue of the effects of its variations. However, local sensitivity analysis could only deal with small perturbations and allowed single parameter to vary, which was not so practical in reality. MPSA has been

therefore adopted to evaluate the model with respect to multiple parameters. In the study, calcium uptake, PLC_G/PIP_2, and Ca^{2+}/CaM rate constants have been determined to be more sensitive because their correlation coefficients were relatively small.

We have shown that PLC–Ca^{2+} was involved in regulating melanoma-induced VE-cadherin disassembly. Under an assumption that $[Ca^{2+}]_i$ response is required and directly proportional to junction changes, the model has described the relative importance of k_3 associated with PLC, in good agreement with the experimental observations. However, the model has not yet been completely developed until the initial concentrations of the variables are supplied. In addition, future studies are needed to provide information on which receptors/ligands activate the GPCR-mediated signaling pathway, and to identify potential signaling molecules that link PKC to EC junction regulation, in order to glean a fuller picture for the input and output of the signaling model.

Current experimental techniques allow us to directly assess biological functions, and the computational approach can be complementary for unraveling the underlying complexity. Our current understanding of calcium mobilization in endothelial cells during their interaction with tumors is very limited. Thus the mathematical model simulating calcium responses in such context may aid us in deciphering the cancer-related signaling mechanisms in its microenvironment in the processes of transformation and metastasis.

APPENDICES

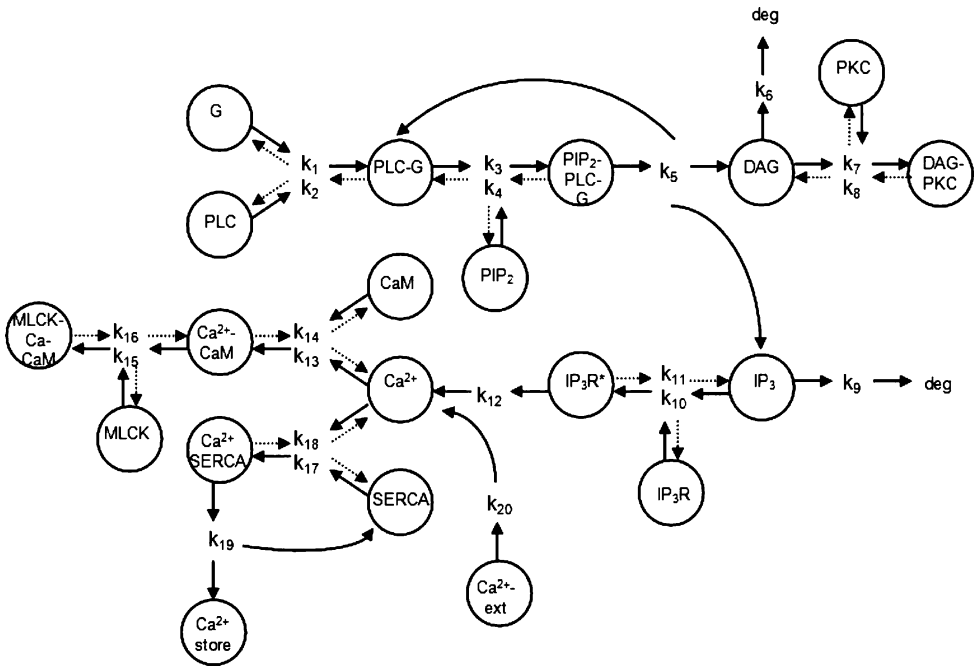

APPENDIX A. A graphical representation of calcium signaling model.

APPENDIX B

$$\frac{d\mathrm{G}}{dt} = -k_1 \cdot \mathrm{G} \cdot \mathrm{PLC} + k_2 \cdot \mathrm{PLC\_G}$$

$$\frac{d\mathrm{PLC}}{dt} = -k_1 \cdot \mathrm{G} \cdot \mathrm{PLC} + k_2 \cdot \mathrm{PLC\_G}$$

$$\frac{d\mathrm{PLC\_G}}{dt} = k_1 \cdot \mathrm{G} \cdot \mathrm{PLC} - k_2 \cdot \mathrm{PLC\_G} - k_3 \cdot \mathrm{PLC\_G} \cdot \mathrm{PIP_2} + k_4 \cdot \mathrm{PIP_2\_PLC\_G} + k_5 \cdot \mathrm{PIP_2\_PLC\_G}$$

$$\frac{d\mathrm{PIP_2}}{dt} = -k_3 \cdot \mathrm{PLC\_G} \cdot \mathrm{PIP_2} + k_4 \cdot \mathrm{PIP_2\_PLC\_G}$$

$$\frac{d\mathrm{PIP_2\_PLC\_G}}{dt} = k_3 \cdot \mathrm{PLC\_G} \cdot \mathrm{PIP_2} - k_4 \cdot \mathrm{PIP_2\_PLC\_G} - k_5 \cdot \mathrm{PIP_2\_PLC\_G}$$

$$\frac{d\mathrm{DAG}}{dt} = k_5 \cdot \mathrm{PIP_2\_PLC\_G} - k_6 \cdot \mathrm{DAG} - k_7 \cdot \mathrm{DAG} \cdot \mathrm{PKC} + k_8 \cdot \mathrm{DAG\_PKC}$$

$$\frac{d\mathrm{IP_3}}{dt} = k_5 \cdot \mathrm{PIP_2\_PLC\_G} - k_9 \cdot \mathrm{IP_3} - 3 \cdot k_{10} \cdot \mathrm{IP_3^3} \cdot \mathrm{IP_3R} + 3 \cdot k_{11} \cdot \mathrm{IP_3R^*}$$

$$\frac{d\mathrm{PKC}}{dt} = -k_7 \cdot \mathrm{DAG} \cdot \mathrm{PKC} + k_8 \cdot \mathrm{DAG\_PKC}$$

$$\frac{d\mathrm{DAG\_PKC}}{dt} = k_7 \cdot \mathrm{DAG} \cdot \mathrm{PKC} - k_8 \cdot \mathrm{DAG\_PKC}$$

$$\frac{d\mathrm{IP_3R}}{dt} = -k_{10} \cdot \mathrm{IP_3^3} \cdot \mathrm{IP_3R} + k_{11} \cdot \mathrm{IP_3R^*}$$

$$\frac{d\mathrm{IP_3R^*}}{dt} = k_{10} \cdot \mathrm{IP_3^3} \cdot \mathrm{IP_3R} - k_{11} \cdot \mathrm{IP_3R^*} - k_{12} \cdot \mathrm{IP_3R^*}$$

$$\frac{d\mathrm{Ca^{2+}}}{dt} = k_{12} \cdot \mathrm{IP_3R^*} - 4 \cdot k_{13} \cdot \mathrm{Ca^{2+}}^4 \cdot \mathrm{CaM} + 4 \cdot k_{14} \cdot \mathrm{Ca^{2+}\_CaM} - k_{17} \cdot \mathrm{Ca^{2+}} \cdot \mathrm{SERCA} + k_{18} \cdot \mathrm{Ca^{2+}\_SERCA} + k_{20} \cdot \mathrm{Ca^{2+}\_ext}$$

$$\frac{d\mathrm{CaM}}{dt} = -k_{13} \cdot \mathrm{Ca^{2+}}^4 \cdot \mathrm{CaM} + k_{14} \cdot \mathrm{Ca^{2+}\_CaM}$$

$$\frac{d\mathrm{Ca^{2+}\_CaM}}{dt} = k_{13} \cdot \mathrm{Ca^{2+}}^4 \cdot \mathrm{CaM} - k_{14} \cdot \mathrm{Ca^{2+}\_CaM} - k_{15} \cdot \mathrm{Ca^{2+}\_CaM} \cdot \mathrm{MLCK} + k_{16} \cdot \mathrm{MLCK\_Ca\_CaM}$$

$$\frac{d\mathrm{MLCK}}{dt} = -k_{15} \cdot \mathrm{Ca^{2+}\_CaM} \cdot \mathrm{MLCK} + k_{16} \cdot \mathrm{MLCK\_Ca\_CaM}$$

$$\frac{d\mathrm{MLCK\_Ca\_CaM}}{dt} = k_{15} \cdot \mathrm{Ca^{2+}\_CaM} \cdot \mathrm{MLCK} - k_{16} \cdot \mathrm{MLCK\_Ca\_CaM}$$

$$\frac{d\mathrm{SERCA}}{dt} = -k_{17} \cdot \mathrm{Ca^{2+}} \cdot \mathrm{SERCA} + k_{18} \cdot \mathrm{Ca^{2+}\_SERCA} + k_{19} \cdot \mathrm{Ca^{2+}\_SERCA}$$

$$\frac{d\mathrm{Ca^{2+}\_SERCA}}{dt} = k_{17} \cdot \mathrm{Ca^{2+}} \cdot \mathrm{SERCA} - k_{18} \cdot \mathrm{Ca^{2+}\_SERCA} - k_{19} \cdot \mathrm{Ca^{2+}\_SERCA}$$

$$\frac{d\mathrm{Ca^{2+}\ store}}{dt} = k_{19} \cdot \mathrm{Ca^{2+}\_SERCA}$$

$$\frac{d\mathrm{Ca^{2+}\_ext}}{dt} = -k_{20} \cdot \mathrm{Ca^{2+}\_ext}$$

APPENDIX C. Summary of parameter values.

Parameter	Description	Value	Unit
k_1	G protein/PLC association	2.52	$\mu M^{-1}\ s^{-1}$
k_2	G protein/PLC dissociation	1	s^{-1}
k_3	PLC_G/PIP_2 association	0.83	$\mu M^{-1}\ s^{-1}$
k_4	PLC_G/PIP_2 dissociation	0.1	s^{-1}
k_5	PIP_2_PLC_G → DAG + IP_3	0.58	s^{-1}
k_6	DAG → deg	0.15	s^{-1}
k_7	DAG/PKC association	0.0079998	$\mu M^{-1}\ s^{-1}$
k_8	DAG/PKC dissociation	8.6348	s^{-1}
k_9	IP_3 → deg	2.5	s^{-1}
k_{10}	IP_3/IP_3R association	0.0022	$\mu M^{-3}\ s^{-1}$
k_{11}	IP_3/IP_3R dissociation	1	s^{-1}
k_{12}	IP_3R → Ca^{2+}	2.5	s^{-1}
k_{13}	Ca^{2+}/CaM association	0.465	$\mu M^{-4}\ s^{-1}$
k_{14}	Ca^{2+}/CaM dissociation	10	s^{-1}
k_{15}	Ca^{2+}_CaM/MLCK association	28	$\mu M^{-1}\ s^{-1}$
k_{16}	Ca^{2+}_CaM/MLCK dissociation	0.0308	s^{-1}
k_{17}	Ca^{2+}/SERCA association	0.003	$\mu M^{-1}\ s^{-1}$
k_{18}	Ca^{2+}/SERCA dissociation	288	s^{-1}
k_{19}	Ca^{2+} → Ca^{2+} store	72	s^{-1}
k_{20}	Ca^{2+}_ext → Ca^{2+}	0.005	s^{-1}

APPENDIX D. Summary of initial concentrations of the variables.

Variable	Initial concentration (μM)
G protein	18
PLC	18
PLC_G	0
PIP_2	18
PIP_2_PLC_G	0
DAG	0
IP_3	0
PKC	1
DAG_PKC	0
IP_3R	10
IP_3R*	0
Ca^{2+}	0.18
CaM	0.4
Ca^{2+}_CaM	0
MLCK	1
MLCK_Ca_CaM	0
SERCA	10
Ca^{2+}_SERCA	0
Ca^{2+} store	0
Ca^{2+}_ext	0.1

IP_3R* denotes active form of IP_3R.

ACKNOWLEDGMENTS

This work was supported by NIH-CA97306 and CA-125707.

REFERENCES

[1]Bhalla, U. S. Mechanisms for temporal tuning and filtering by postsynaptic signaling pathways. *Biophys. J.* 83:740–752, 2002.

[2]Bhalla, U. S., and R. Iyengar. Emergent properties of networks of biological signaling pathways. *Science* 283:381–387, 1999.

[3]Campagne, F., S. Neves, C. W. Chang, L. Skrabanek, P. T. Ram, R. Iyengar, and H. Weinstein. Quantitative information management for the biochemical computation of cellular networks. *Sci. STKE* 248:pl11, 2004.

[4]Cho, K.-H., S.-Y. Shin, W. Kolch, and O. Wolkenhauer. Experimental design in systems biology, based on parameter sensitivity analysis. using a monte carlo method: a case study for the TNF a-mediated NF-kB signal transduction. *Simulation* 79:726–739, 2003.

[5]Fink, C. C., B. Slepchenko, and L. M. Loew. Determination of time-dependent inositol-1,4,5-trisphosphate concentrations during calcium release in a smooth muscle cell. *Biophys. J.* 77:617–628, 1999.

[6]Grynkiewicz, G., M. Poenie, and R. Y. Tsien. A new generation of Ca^{2+} indicators with greatly improved fluorescence properties. *J. Biol. Chem.* 260:3440–3450, 1985.

[7]Huang, A. J., J. E. Manning, T. M. Bandak, M. C. Ratau, K. R. Hanser, and S. C. Silberstein. Endothelial cell cytosolic free calcium regulates neutrophil migration across monolayers of endothelial cells. *J. Cell Biol.* 120:1371–1380, 1993.

[8]Jordan, J. D., E. M. Landau, and R. Iyengar. Signaling networks: the origins of cellular multitasking. *Cell* 103:193–200, 2000.

[9]Lukas, T. J. A signal transduction pathway model prototype I: From agonist to cellular endpoint. *Biophys. J.* 87:1406–1416, 2004.

[10]Marchant, J. S., and C. W. Taylor. Cooperative activation of IP3 receptors by sequential binding of IP_3 and Ca^{2+} safeguards against spontaneous activity. *Curr. Biol.* 7:510–518, 1997.

[11]Nwariaku, F. E., J. Chang, X. Zhu, Z. Liu, S. L. Duffy, N. H. Halaihel, L. Terada, and R. H. Turnage. The role of p38 MAP kinase in tumor necrosis factor-induced redistribution of vascular endothelial cadherin and increased endothelial permeability. *Shock* 18:82–85, 2002.

[12]Peng, H.-H., L. Hodgson, A. J. Henderson, and C. Dong. Involvement of phospholipase C signaling in melanoma cell-induced endothelial junction disassembly. *Front. Biosci.* 10:1597–1606, 2005.

[13]Sandoval, R., A. B. Malik, R. D. Minshall, P. Kouklis, C. A. Ellis, and C. Tiruppathi. Ca(2+) signalling and PKCalpha activate increased endothelial permeability by disassembly of VE-cadherin junctions. *J. Physiol.* 533:433–445, 2001.

[14]Siflinger-Birnboim, A., H. Lum, P. J. Del Vecchio, and A. B. Malik. Involvement of Ca^{2+} in the H_2O_2-induced increase in endothelial permeability. *Am. J. Physiol. Lung Cell. Mol. Physiol.* 270:L973–L978, 1996.

[15]Sivakumaran, S., S. Hariharaputran, J. Mishra, and U. S. Bhalla. The Database of Quantitative Cellular Signaling: management and analysis of chemical kinetic models of signaling networks. *Bioinformatics* 19:408–415, 2003.

[16]Wong, C. K., C. B. Wang, W. K. Ip, Y. P. Tian, and C. W. K. Lam. Role of p38 MAPK and NF-kB for chemokine release in coculture of human eosinophils and bronchial epithelial cells. *Clin. Exp. Immunol.* 139:90–100, 2005.